0026-895X/06/7001-194–205$20.00
MOLECULAR PHARMACOLOGY
Copyright © 2006 The American Society for Pharmacology and Experimental Therapeutics
Mol Pharmacol 70:194–205, 2006

Vol. 70, No. 1
22616/3124635
Printed in U.S.A.

Analysis of G Protein $\beta\gamma$ Dimer Formation in Live Cells Using Multicolor Bimolecular Fluorescence Complementation Demonstrates Preferences of β_1 for Particular γ Subunits

Stacy M. Mervine, Evan A. Yost, Jonathan L. Sabo, Thomas R. Hynes, and Catherine H. Berlot

Weis Center for Research, Geisinger Clinic, Danville, Pennsylvania

Received January 18, 2006; accepted April 26, 2006

ABSTRACT

The specificity of G protein $\beta\gamma$ signaling demonstrated by in vivo knockouts is greater than expected based on in vitro assays of $\beta\gamma$ function. In this study, we investigated the basis for this discrepancy by comparing the abilities of seven $\beta_1\gamma$ complexes containing γ_1, γ_2, γ_5, γ_7, γ_{10}, γ_{11}, or γ_{12} to interact with α_s and of these γ subunits to compete for interaction with β_1 in live human embryonic kidney (HEK) 293 cells. $\beta\gamma$ complexes were imaged using bimolecular fluorescence complementation, in which fluorescence is produced by two nonfluorescent fragments (N and C) of cyan fluorescent protein (CFP) or yellow fluorescent protein (YFP) when brought together by proteins fused to each fragment. Plasma membrane targeting of α_s-CFP varied inversely with its expression level, and the abilities of YFP-N-β_1YFP-C-γ complexes to increase this targeting varied by 2-fold or less. However, there were larger differences in the abilities of the CFP-N-γ subunits to compete for association with CFP-C-β_1. When the intensities of coexpressed CFP-C-β_1CFP-N-γ (cyan) and CFP-C-β_1YFP-N-γ_2 (yellow) complexes were compared under conditions in which CFP-C-β_1 was limiting, the CFP-N-γ subunits exhibited a 4.5-fold range in their abilities to compete with YFP-N-γ_2 for association with CFP-C-β_1. CFP-N-γ_{12} and CFP-N-γ_1 were the strongest and weakest competitors, respectively. Taken together with previous demonstrations of a role for $\beta\gamma$ in the specificity of receptor signaling, these results suggest that differences in the association preferences of coexpressed β and γ subunits for each other can determine which complexes predominate and participate in signaling pathways in intact cells.

Cells integrate multiple receptor-G protein pathways to respond to stimulation by hormones and neurotransmitters. Given the numerous mammalian G protein isoforms (23 α subunits, 5 β subunits, and 12 γ subunits), maintenance of signaling specificity is clearly a vital cellular function. α subunits have been thought to play the most important role in specificity because they exhibit greater diversity in their interactions with receptors and effectors than do the different $\beta\gamma$ complexes when tested in vitro (Clapham and Neer, 1997; Robishaw and Berlot, 2004). However, in vivo knockout experiments have demonstrated unique functions for particular $\beta\gamma$ complexes. For instance, mice containing targeted deletions of either γ_7 (Schwindinger et al., 2003) or γ_3 (Schwindinger et al., 2004) exhibit distinct phenotypes. Moreover, ribozyme-mediated depletion of γ_7 in HEK-293 cells results in a corresponding decrease in the level of β_1 (Wang et al., 1999) and γ_7-knockout mice express reduced levels of α_{olf} (Schwindinger et al., 2003), suggesting that associations of particular subunits may be obligatory for their stability. The basis for this discrepancy in $\beta\gamma$ specificity in vivo versus in vitro is not well understood.

G protein signaling specificity is most likely maintained at multiple levels, including cell-type–specific expression, subcellular localization, and protein-protein interactions (Robishaw and Berlot, 2004). Only a subset of the genes encoding G protein-coupled receptors and G protein subunits is expressed in individual cells, and their expression levels can change during development with functional consequences (Iiri et al., 1995). Subcellular compartmentalization of G proteins and receptors may facilitate or impair interactions between coexpressed proteins (Ostrom, 2002). At the molecular level, reconstitution experiments have indicated differences in the $\alpha\beta\gamma$ combinations that are preferred by particular receptors (Figler et al., 1997; Richardson and Robishaw, 1999; Hou et al., 2000; Lim et al., 2001; McIntire et al., 2001).

Herein, we focus on subcellular regulation of $\beta\gamma$ signaling

This work was supported by National Institutes of Health grant GM50369.
Article, publication date, and citation information can be found at http://molpharm.aspetjournals.org.
doi:10.1124/mol.106.022616.

ABBREVIATIONS: HEK, human embryonic kidney; BiFC, bimolecular fluorescence complementation; YFP, yellow fluorescent protein; CFP, cyan fluorescent protein; ECFP, enhanced cyan fluorescent protein; mRFP, monomeric red fluorescent protein; Cer, monomeric cerulean protein.

specificity. Among the potential regulatory mechanisms are preferential associations of β and γ subunits, of α subunits with $\beta\gamma$ complexes, and of $\alpha\beta\gamma$ combinations with G protein-coupled receptors. Based on studies using the yeast two-hybrid system (Yan et al., 1996) and reticulocyte lysates (Schmidt et al., 1992; Ray et al., 1995; Dingus et al., 2005), most β and γ subunits can form complexes. However, because the cellular environment can affect $\beta\gamma$ assembly (Clapham and Neer, 1997; Lukov et al., 2005; Li et al., 2006), it would be optimal to study dimerization in vivo. In addition, because cells express multiple isoforms of β and γ subunits, determining the relative preferences of the subunits for each other in intact cells would help to predict which complexes are most likely to form in vivo.

To study $\beta\gamma$ assembly in live cells, we have applied the strategy of BiFC (Hu et al., 2002) to localize and compare the relative amounts of different $\beta\gamma$ dimers (Hynes et al., 2004b). This approach involves the production of a fluorescent signal by two nonfluorescent fragments of CFP or YFP (N and C) when they are brought together by interactions between proteins fused to each fragment. This makes it possible to image $\beta\gamma$ complexes exclusively, rather than individual β and γ subunits. By imaging the fluorescent signals formed by pairwise combinations of β_1, β_2, and β_5 with γ_1, γ_2, and γ_7 (Hynes et al., 2004b), we found that β can direct trafficking of γ. In addition we found that upon stimulation of the β_2-adrenergic receptor, both α_s-CFP and YFP-N-β_1YFP-C-γ_7 internalize from the plasma membrane to the cytoplasm and colocalize on vesicles (Hynes et al., 2004a).

In this report, we compare the abilities of seven different $\beta_1\gamma$ complexes to interact with α_s and of these γ subunits to compete for interaction with β_1 in live HEK-293 cells. Interaction of α_s with $\beta\gamma$ was measured using a plasma membrane targeting assay. Plasma membrane targeting of α_s-CFP varied inversely with its expression level, and the abilities of YFP-N-β_1YFP-C-γ complexes to increase this targeting varied by 2-fold or less. To compare the interactions of different γ subunits with β_1, we produced CFP-C-β_1, YFP-N-γ_2, and CFP-N-γ subunits. When the intensities of coexpressed CFP-C-β_1CFP-N-γ (cyan) and CFP-C-β_1YFP-N-γ_2 (yellow) complexes were compared under conditions in which CFP-C-β_1 was limiting, the CFP-N-γ subunits exhibited a 4.5-fold range in their abilities to compete with YFP-N-γ_2 for association with CFP-C-β_1. Taken together with previous demonstrations of a role for $\beta\gamma$ in the specificity of receptor signaling, these results suggest that differences in association preferences of coexpressed β and γ subunits may determine which complexes predominate and participate in cellular signaling pathways.

Materials and Methods

Production of Fluorescent Fusion Proteins. YFP(1–158)β_1, YFP(159–238)γ_1, YFP(159–238)γ_2, and YFP(159–238)γ_7 were produced as described previously (Hynes et al., 2004b). To produce YFP(159–238)γ_5, YFP(159–238)γ_{10}, YFP(159–238)γ_{11}, and YFP(159–238)γ_{12}, the bovine γ_5 cDNA, the human γ_{10} cDNA, the bovine γ_{11} cDNA, and the human γ_{12} cDNA (obtained from Janet Robishaw, Weis Center for Research, Danville, PA) were each amplified by a PCR that added a BamHI site and a linker sequence (Arg-Ser) to the 5′ end and a BglII site to the 3′ end, digested with BamHI and BglII, and subcloned into the BglII site of YFP(159–238)pcDNAI/Amp, as described previously (Hynes et al., 2004b), so that YFP(159–238) was fused to the amino terminus of each of the γ subunit cDNAs.

To produce CFP(159–238)β_1 in pcDNAI/Amp, CFP(159–238) was amplified by a PCR from ECFP (Clontech, Mountain View, CA) containing a substitution of His for Asn-164. The PCR introduced a BamHI site at the 5′ end of CFP(159–238) and a BglII site at the 3′ end. A BglII site was introduced into the polylinker of pcDNAI/Amp (Invitrogen, Carlsbad, CA) 3′ to the BamHI site and CFP(159–238) was subcloned into these sites to produce CFP(159–238)pcDNAI/Amp. A BglII site in the human β_1 cDNA (obtained from Janet Robishaw) was removed using the QuikChange site-directed mutagenesis kit (Stratagene, La Jolla, CA), and the cDNA was amplified by a PCR that added a linker sequence (Arg-Ser-Ile-Ala-Thr) containing a BamHI site on the 5′ end and a BglII site on the 3′ end. This PCR product was digested with BamHI and BglII and subcloned into the BglII site of CFP(159–238)pcDNAI/Amp so that CFP(159–238) was fused to the amino terminus of β_1.

To produce CFP(1–158)γ constructs in pcDNAI/Amp, CFP(1–158) was amplified by a PCR from ECFP (Clontech) that introduced a BamHI site at the 5′ end and a BglII site at the 3′ end and subcloned into the BamHI and BglII sites of the modified pcDNAI/Amp vector described above to produce CFP(1–158)pcDNAI/Amp. Each of the γ subunit cDNAs was amplified by a PCR, as described above for the YFP(159–238)γ constructs, digested with BamHI and BglII, and subcloned into the BglII site of CFP(1–158)pcDNAI/Amp so that CFP(1–158) was fused to the amino terminus of each of the γ subunits. Cer(1–158)γ constructs in pcDNAI/Amp were produced in the same way, using monomeric Cerulean (Rizzo et al., 2004) (obtained from David Piston, Vanderbilt University, Nashville, TN), which contains S72A, Y145A, H148D, and A206K substitutions in ECFP, as the PCR template.

mRFP-Mem was constructed by a fusion PCR using pEYFP-Mem (Clontech) and mRFP1/pcDNA3 (obtained from Roger Tsien, University of California, San Diego) as templates. The PCR product contained the first 20 residues of neuromodulin fused to the amino terminus of mRFP and had a unique 5′ BglII site and 3′ NotI site. This PCR product was digested with BglII and NotI and subcloned into BglII/NotI digested pEYFP-Mem.

Imaging of Transfected Cells. HEK-293 cells (American Type Culture Collection, Manassas, VA) were plated at a density of 2×10^5 cells per well on four-well chambered coverslips (Lab-Tek II; Nalge Nunc, Naperville, IL). On the following day, the cells were transiently transfected using 0.25 μl of LipofectAMINE 2000 Reagent (Invitrogen). Plasmids were transfected using the following amounts: α_s-CFP, 0.15 μg or as described in the legend to Fig. 1; YFP-N-β_1, YFP-C-γ subunits, CFP-C-β_1, CFP-N-γ subunits, YFP-N-γ_2, CFP-N, and CFP-C, 0.075 μg; and YFP and mRFP-Mem, 0.0025 μg. The cells were imaged 2 days after transfection at 63× using a Zeiss Axiovert 200 fluorescence microscope equipped with computer-controlled filter wheels, shutters, xyz stage (Ludl, Hawthorne, NY), and ORCA-ER camera (Hamamatsu Corporation, Bridgewater, NJ), under the control of IPLab software (Scanalytics, Inc., Fairfax, VA). A single triple-pass dichroic mirror (86006bs; Chroma, Brattleboro, VT) was used to ensure image registration. Excitation and emission band-pass filters for CFP (430/25, 465/30), YFP (495/20, 535/25), and mRFP1 (565/25, 630/60) were obtained from Chroma. One hour before imaging the culture medium was replaced with 20 mM HEPES-buffered minimal essential medium with Earle's salts without bicarbonate. During imaging, the cells were maintained at 37°C using a CSMI stage incubator (Harvard Apparatus, Holliston, MA).

Image Analysis. The membrane marker mRFP-Mem was included in all transfections and was used as the primary criterion for selecting cells for imaging and analysis. Cells having a clear plasma membrane border and adjacent region of cytoplasm were identified. If the cell also had detectable intensity of the CFP and/or YFP labeled proteins that were also transfected, then the cell image was recorded. Exposure times for each color varied depending on cell intensity, and the following corrections were made so that the inten-

sity values correspond to a 1-s exposure with image background subtracted. The background intensity for each image was determined by averaging the intensity of a region of pixels outside the cell. The image background was subtracted from each image, and the remaining intensity was scaled to correspond to an exposure time of 1 s. To eliminate the effect of day-to-day variation in lamp intensity, an additional correction was applied based on images of a slide containing a mixture of blue-green, yellow-green, and red FluoSphere 1-μm beads (Invitrogen) that were taken each day. A small amount of bleed-through of CFP intensity into the YFP images (0.6%) was then subtracted. All image processing was performed using IPlab software.

The average fluorescence intensity of each cell was determined by tracing a border around the edge of the cell in the mRFP-Mem image using a Cintiq pen-based display screen (Wacom, Vancouver, WA). The average pixel intensity of the entire cell including the border was calculated for each color.

The plasma membrane fraction is a measurement of the distribution of a labeled protein between the plasma membrane and cytoplasmic compartments. The plots in Fig. 1A illustrate the pixel intensity values for the membrane marker (mRFP-Mem) and cytoplasm marker (YFP) along the white line drawn perpendicular to the plasma membrane in the mRFP-Mem image. Plasma membrane pixels (black line) corresponding to a length of plasma membrane were identified and marked using the mRFP-Mem image. Cytoplasm pixels (black box) were marked with a 12 × 12 pixel box adjacent to the plasma membrane pixels in a region that was devoid of labeled intracellular vesicles or membranes. The plasma membrane to cytoplasm ratios of labeled G protein subunits (ProteinRatio), plasma membrane marker (MemRatio), and cytoplasm marker (CytoRatio)

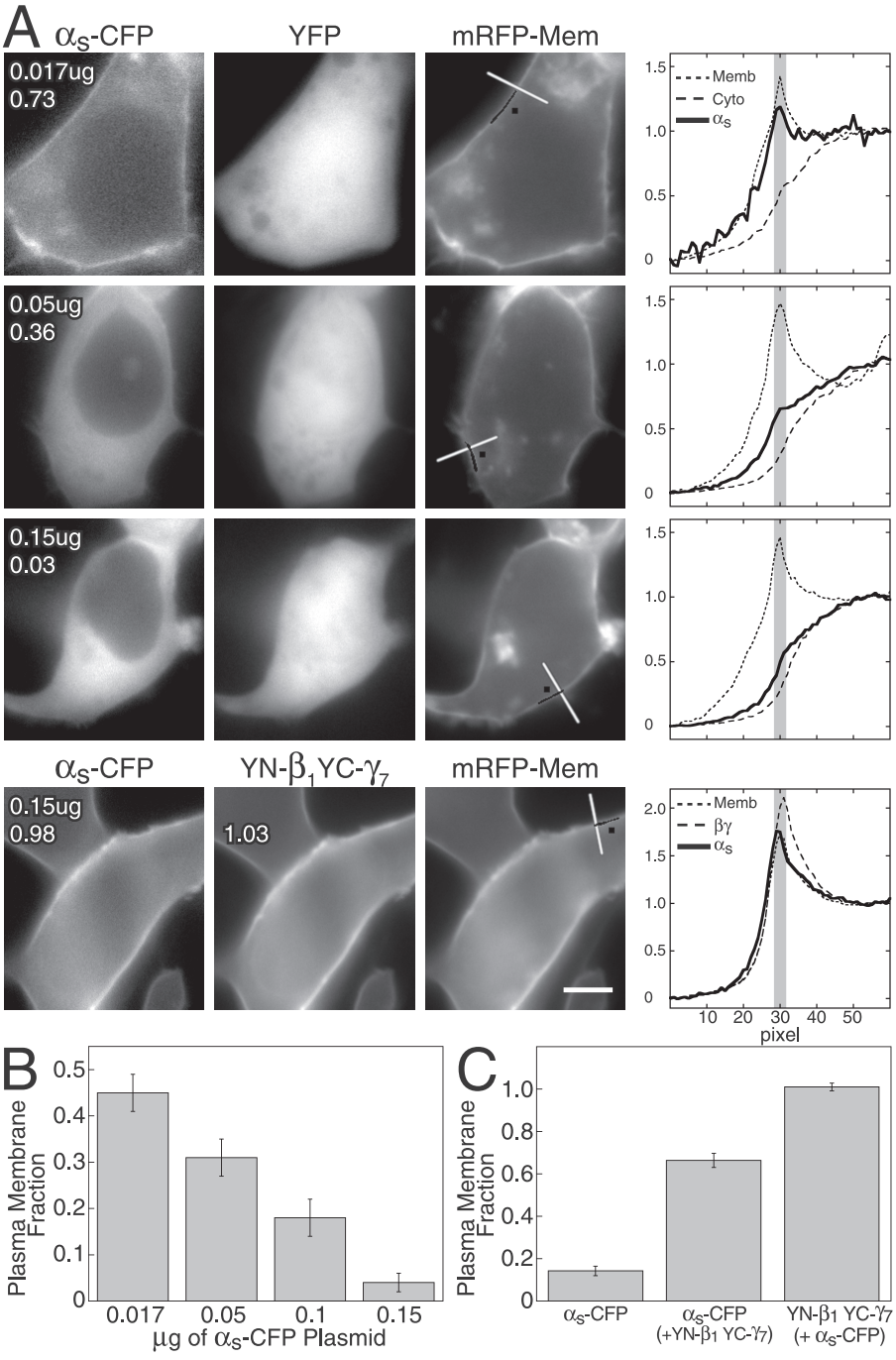

Fig. 1. Targeting of α_s-CFP to the plasma membrane is plasmid dose-dependent and can be increased by coexpression with YFP-N-β_1YFP-C-γ_7. A, left, representative images of α_s-CFP in HEK-293 cells transfected with the indicated amounts of α_s-CFP-expressing plasmid. The cells were also transfected with mRFP-Mem, a plasma membrane marker, and either YFP, a cytoplasm marker, or YFP-N-β_1 and YFP-C-γ_7, as indicated. The plasma membrane fractions (determined as described under *Materials and Methods*) of α_s-CFP for each cell and for YFP-N-β_1YFP-C-γ_7 in the bottom cell are listed. The black line and black square on the mRFP-Mem image indicate the pixels used in the measurements of average membrane and cytoplasm intensity. YN indicates YFP-N and YC indicates YFP-C. Scale bar, 5 μm. Right, graphs show the intensities of each of the three signals along the white line drawn on the mRFP-Mem image from the outside of the cell into the cytoplasm. The location of the plasma membrane is highlighted in gray. The intensity values for each color were scaled to a value of one in the cytoplasm region. B, plasma membrane fractions of α_s-CFP in cells transfected with the indicated amounts of α_s-CFP plasmid. Values represent the mean ± S.E. The number of cells analyzed for each condition was as follows: 0.017 μg of plasmid, 61; 0.05 μg of plasmid, 64; 0.1 μg of plasmid, 38; 0.15 μg of plasmid, 60. C, plasma membrane fractions of α_s-CFP (first and second bars) and YFP-N-β_1YFP-C-γ_7 (third bar) in cells transfected with 0.15 μg of α_s-CFP plasmid in the absence (185 cells) or presence (144 cells) of 0.075 μg each of plasmids expressing YFP-N-β_1 and YFP-C-γ_7. Values represent the mean ± S.E.

were calculated by dividing the average intensity of each label in the marked plasma membrane region by the average intensity in the marked cytoplasm region. Based on images of cells transfected with YFP, mRFP-Mem, and α_s-CFP (Fig. 1A), the CytoRatio was very consistent from cell to cell, with a mean value of 0.62 (S.E. = 0.01, n = 223). Because most of the experiments described here required both the CFP and YFP color channels for labeled G protein subunits, the average CytoRatio of 0.62 was used in the calculations of plasma membrane fraction. The plasma membrane fraction of a labeled protein is defined as the plasma membrane to cytoplasm ratio of the protein relative to that of the plasma membrane and cytoplasm markers, and was calculated using the following equation: Plasma Membrane Fraction(Protein) = (ProteinRatio − CytoRatio)/(MemRatio − CytoRatio). A value of zero corresponds to a completely cytoplasmic distribution, and a value of one corresponds to a completely plasma membrane distribution.

To determine the average cellular intensity of α_s-CFP at which its plasma membrane fraction was half-maximal in the absence or presence of a YFP-N-β_1YFP-C-γ complex (Fig. 2A, Table 1), the plasma membrane fraction of α_s-CFP was fitted to the equation $Y = b + (a - b)/[1 + (X/c)^d]$, where X is the average intensity of α_s-CFP, Y is the observed plasma membrane fraction of α_s-CFP, a is the maximum plasma membrane fraction of α_s-CFP, b is the minimum plasma membrane fraction of α_s-CFP, c is the average intensity of α_s-CFP at which its plasma membrane fraction is half-maximal, and d is the slope factor. S.E. of the fits were determined by Kaleidograph (Synergy Software, Reading, PA).

To determine the YFP-N-β_1YFP-C-γ/α_s-CFP intensity ratio at which the plasma membrane fraction of α_s-CFP was half-maximal (Fig. 2B, Table 1), the plasma membrane fraction of α_s-CFP was fitted to the same equation, $Y = b + (a - b)/[1 + (X/c)^d]$, where X is the YFP-N-β_1YFP-C-γ/α_s-CFP intensity ratio, Y is the observed plasma membrane fraction of α_s-CFP, a = 0, b = 1, c is the YFP-N-β_1YFP-C-γ/α_s-CFP intensity ratio at which the plasma membrane targeting of α_s-CFP is half-maximal, and d is the slope factor. S.E. of the fits were determined by Kaleidograph.

Measurement of Fluorescence in Cell Populations. HEK-293 cells (1.6×10^6 per 60-mm dish) were transfected with plasmids as described in the legends to Figs. 5 and 6 using 6 μl of Lipofectamine 2000 Reagent (Invitrogen) according to the manufacturer's instructions. Two days later, cells were washed once in 4 ml of HEPES-buffered salt solution + $CaCl_2$ media (20 mM HEPES, pH 7.2, 118 mM NaCl, 4.6 mM KCl, 10 mM D-glucose, and 1 mM $CaCl_2$). HEPES-buffered salt solution + EDTA media (2 ml; 20 mM HEPES, pH 7.2, 118 mM NaCl, 4.6 mM KCl, 10 mM D-glucose, and 0.5 mM EDTA) were then added to the dish, cells were scraped off the dishes with a rubber policeman, triturated with a pipet to break up clumps, and suspended in a 1-cm square glass cuvette with a magnetic stir bar.

Data were collected on a PC1 photon-counting spectrofluorometer (ISS, Champaign, IL) configured with motorized filter wheels on both the excitation path between the excitation monochrometer and the sample and on the emission path between the sample and the emission monochrometer. The slits on the excitation and emission monochrometers were set to 16 nm. To eliminate the light scattering signal from the cell suspensions during measurements of CFP and YFP intensity, band-pass filters were used in the excitation filter wheel in combination with long-pass filters in the emission filter wheel. For CFP measurements, the excitation monochrometer was set to 430 nm with a 430/25 band-pass filter, and the emission monochrometer was set to 480 nm with a 455 long-pass filter. For YFP measurements the excitation was set to 492 nm with a 492/18 band-pass filter, and emission was set to 530 nm with a 515 long-pass filter.

The cell density of each sample was determined from a light-scattering measurement at 650 nm. Excitation and emission monochrometers were set to 650 nm, and a 1.3 OD neutral density filter in combination with a long-pass filter at 590 nm was used in the excitation filter wheel. All filters were from Chroma. To subtract the

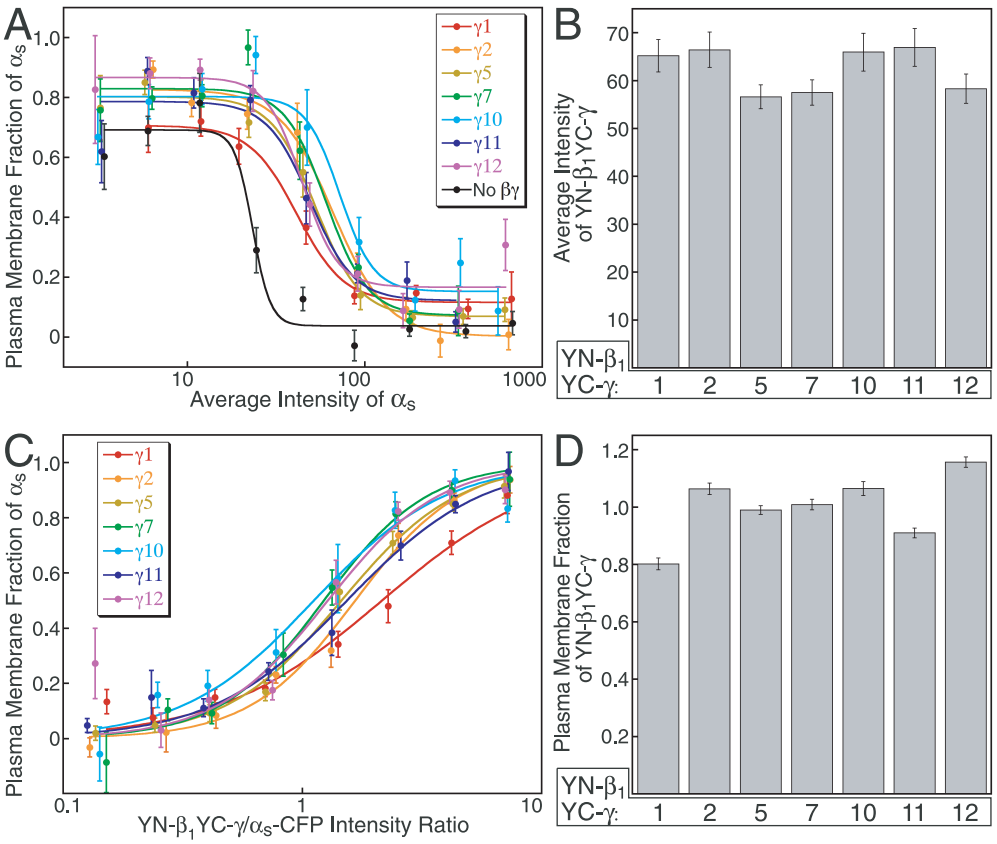

Fig. 2. Targeting of α_s-CFP by YFP-N-β_1YFP-C-γ complexes. HEK-293 cells were transfected with α_s-CFP, YFP-N-β_1, and a YFP-C-γ subunit as described under *Materials and Methods*. A, plot of plasma membrane fraction of α_s-CFP as a function of its intensity in the absence or presence of the indicated YFP-N-β_1YFP-C-γ complexes. B, average intensities of each of the YFP-N-β_1YFP-C-γ complexes coexpressed with α_s-CFP. YN indicates YFP-N and YC indicates YFP-C. C, plot of plasma membrane fraction of α_s-CFP as a function of the ratio of intensities of YFP-N-β_1YFP-C-γ complexes to that of α_s-CFP. D, plasma membrane fractions of each of the YFP-N-β_1YFP-C-γ complexes coexpressed with α_s-CFP. All data were derived from the same cell images for each YFP-N-β_1YFP-C-γ combination. The numbers of cells analyzed were as follows: no $\beta\gamma$ (181), $\beta_1\gamma_1$ (111), $\beta_1\gamma_2$ (132), $\beta_1\gamma_5$ (168), $\beta_1\gamma_7$ (142), $\beta_1\gamma_{10}$ (120), $\beta_1\gamma_{11}$ (145), and $\beta_1\gamma_{12}$ (155). In A and C, measurements from individual cells were sorted into equal size bins along the logarithmic x-axis and averaged. Bins containing fewer than three measurements were omitted. All values represent the means ± S.E.

signal that was attributable to autofluorescence, measurements of CFP, YFP, and light scattering were made each day on a dilution series of cells transfected with vector alone. The linear relationship between the autofluorescence signal in the CFP and YFP channels and the light-scattering signal was calculated. The light-scattering measurement of samples containing fluorescent proteins was used to calculate the amount of autofluorescence to subtract from the CFP and YFP measurements. Control of the monochrometers, motorized filter wheels, and data acquisition was done using the Vinci software program (ISS) and allowed the measurements of CFP, YFP, and light scattering to be made in quick succession without repositioning the sample.

In multicolor BiFC experiments, the IC_{50} for inhibition of association of YFP-N-γ_2 with CFP-C-β_1 by Cer-N-γ subunits was defined as micrograms of Cer-N-γ subunit plasmid that produced a 50% decrease in the intensity of CFP-C-β_1YFP-N-γ_2. To determine IC_{50} values, the data were fit to the equation $Y = (a)/[1 + (X/b)^c]$, where X is micrograms of transfected Cer-N-γ plasmid, Y is the amount of fluorescence produced by CFP-C-β_1YFP-N-γ_2, a is the maximum amount of fluorescence produced by CFP-C-β_1YFP-N-γ_2, b is the half-maximal inhibitory concentration (IC_{50}) of the Cer-N-γ subunit, and c is the slope factor. In Table 2, these IC_{50} values were normalized by multiplying by the relative expression levels of the Cer-N-γ subunits (Fig. 5D). The S.E. resulting from the multiplication of IC_{50} ± S.E. by Cer-N-γ expression level ± S.E. was calculated using an equation for error propagation (http://www.rit.edu/~uphysics/uncertainties/Uncertaintiespart2.html).

Membrane Preparations and Immunoblots. HEK-293 cells were transfected as described above for measurement of fluorescence in cell populations, except that 100-mm dishes were used and the number of cells and amounts of plasmids and Lipofectamine 2000 reagent were scaled up accordingly by a factor of 2.78. Forty-eight hours after transfection, membranes were prepared as described previously (Hynes et al., 2004a). Fifty micrograms of membrane proteins were resolved by SDS-polyacrylamide electrophoresis (12.5%), transferred to nitrocellulose, and probed with a polyclonal antibody to GFP, Living Colors A.v. Peptide Antibody (Clontech, Mountain View, CA), which is directed against three peptides derived from GFP residues 100 to 238. The antigen-antibody complexes were detected according to the ECL Western blotting protocol (GE Healthcare, Little Chalfont, Buckinghamshire, UK). Chemiluminescence was imaged using a Lumi-Imager (Roche Applied Science, Indianapolis, IN). Bands in the images were quantified using IPLab software. The intensity of a nonspecific band obtained in membranes from cells transfected with vector alone (pcDNAI/Amp) that comigrated with Cer-N-γ_1, Cer-N-γ_2, Cer-N-γ_{11}, and Cer-N-γ_{12}, was subtracted from the intensities of these constructs.

TABLE 1

α_s-CFP intensities and YN-β_1YC-γ/α_s-CFP intensity ratios at which plasma membrane fraction of α_s-CFP is half-maximal (calculated from the data in Fig. 2)

YNβ_1YC-γ	α_s-CFP Intensity	YN-β_1YC-γ/α_s-CFP Intensity Ratio
None	23 ± 7	
γ_1	41 ± 3	2.15 ± 0.20
γ_2	66 ± 7	1.67 ± 0.09
γ_5	53 ± 4	1.46 ± 0.06
γ_7	60 ± 11	1.23 ± 0.08
γ_{10}	72 ± 14	1.12 ± 0.13
γ_{11}	49 ± 11	1.54 ± 0.13
γ_{12}	44 ± 6	1.28 ± 0.21

Results

Plasma Membrane Targeting of α_s-CFP by YFP-N-βYFP-C-γ Complexes Can Be Used to Measure α_S-$\beta\gamma$ Interaction. One potential mechanism for maintaining G protein signaling specificity in vivo is by selectivity in the interactions between the G protein α and $\beta\gamma$ subunits. To investigate whether there are differences among $\beta\gamma$ complexes in their abilities to interact with α_s, we took advantage of the fact that the localization of α_s-CFP in HEK-293 cells, when transiently expressed without exogenous $\beta\gamma$, depended on the amount of transfected plasmid (Fig. 1, A and B). When cells were transfected with 0.017 μg of α_s-CFP-expressing plasmid, distinct plasma membrane labeling was observed (Fig. 1, A and B). However, transfection with increased amounts of α_s-CFP plasmid resulted in proportionately decreased distributions of the label to the plasma membrane (Fig. 1, A and B). Because interaction with $\beta\gamma$ is required for plasma membrane targeting of α_s (Evanko et al., 2000), the simplest explanation for this relationship between α_s-CFP expression level and localization was that insufficient endogenous $\beta\gamma$ limited plasma membrane localization of the higher levels of α_s-CFP. To test for this, we coexpressed α_s-CFP with $\beta_1\gamma_7$, imaged using BiFC, which involves the production of a fluorescent signal by two nonfluorescent fragments of CFP or YFP (N and C) when brought together by interactions between proteins fused to each fragment (Hynes et al., 2004b). Expression of either YFP-N-β_1 or YFP-C-γ_7 separately or YFP-N and YFP-C together does not produce fluorescence (Hynes et al., 2004b). In addition, fluorescence is not obtained upon coexpression of YFP-N-β_2 and YFP-C-γ_1 (Hynes et al., 2004b), consistent with other studies indicating that β_2 and γ_1 do not interact to form a functional dimer (Iniguez-Lluhi et al., 1992; Schmidt et al., 1992). In support of the idea that plasma membrane targeting of over-expressed α_s-CFP required exogenous $\beta\gamma$, coexpression of YFP-N-β_1YFP-C-γ_7

TABLE 2

Competition of CerN-γ subunits with YN-γ_2 for dimerization with CC-β_1 in live HEK-293 cells

Values represent the mean ± S.E. from three experiments.

γ Subunit	CC-β_1CerN-γ Intensity/μg[a]	CerN-γ Expression[b]	IC_{50} (CerN-γ)[c]	Normalized IC_{50}[d]
	($\times 10^{-6}$)	%	μg	($\times 10^{-2}$)
γ_1	1.28 ± 0.20	68 ± 1	0.86 ± 0.06	0.59 ± 0.04
γ_2	2.36 ± 0.27	100	0.17 ± 0.02	0.17 ± 0.02
γ_5	1.30 ± 0.15	46 ± 9	0.60 ± 0.05	0.28 ± 0.06
γ_7	1.84 ± 0.14	74 ± 6	0.28 ± 0.02	0.21 ± 0.02
γ_{10}	1.13 ± 0.11	30 ± 3	1.17 ± 0.05	0.35 ± 0.04
γ_{11}	1.19 ± 0.10	41 ± 14	0.89 ± 0.09	0.37 ± 0.13
γ_{12}	0.83 ± 0.05	21 ± 6	0.61 ± 0.02	0.13 ± 0.04

[a] Calculated from linear fits of CC-β_1CerN-γ intensity per microgram of plasmid from Fig. 5A.
[b] Defined as percentage of CerN-γ_2 expression from Fig. 5D.
[c] Defined as micrograms of CerN-γ plasmid that produced a 50% decrease in the intensity of CC-β_1YN-γ_2, calculated from the data in Fig. 6A as described under *Materials and Methods*.
[d] Defined as IC_{50} × CerN-γ expression.

resulted in plasma membrane localization of α_s-CFP in cells transfected with 0.15 μg of α_s-CFP-expressing plasmid (Fig. 1, A and C), as observed previously (Hynes et al., 2004a). In the absence of coexpressed YFP-N-β_1YFP-C-γ_7, the distribution of α_s-CFP in cells transfected with this amount of plasmid was similar to that of free YFP, used as a cytosolic marker (Fig. 1A).

Seven Different YFP-N-β_1YFP-C-γ Complexes Target α_s-CFP to the Plasma Membrane with Similar Efficacies. We used the above coexpression system to compare the abilities of YFP-N-β_1YFP-C-γ complexes containing γ_1, γ_2, γ_5, γ_7, γ_{10}, γ_{11}, or γ_{12} to target α_s-CFP to the plasma membrane in HEK-293 cells. These complexes were selected for study because β_1 is widely expressed and the β subunits are highly conserved, with the exception of β_5, whereas the γ subunits are more numerous and less well conserved. β_1 (Wang et al., 1999) and each of these γ subunits, except γ_1 (Wang et al., 1997), have been detected at the protein level in HEK-293 cells. γ_1 and γ_{11} are covalently modified by the 15-carbon isoprenoid, farnesyl, whereas the other γ subunits contain the more hydrophobic 20-carbon isoprenoid geranylgeranyl (Wedegaertner et al., 1995).

Targeting of α_s-CFP to the plasma membrane, in cells transfected with 0.15 μg of plasmid, was determined in the absence and presence of each of the YFP-N-β_1YFP-C-γ complexes (Fig. 2A). The α_s-CFP intensities in individual cells were distributed over a 100-fold range. Even in the presence of coexpressed YFP-N-β_1YFP-C-γ complexes, the fraction of α_s-CFP that associated with the plasma membrane decreased as its intensity increased (Fig. 2A). However, coexpression of each of the YFP-N-β_1YFP-C-γ complexes increased the α_s-CFP intensity at which its plasma membrane targeting was half-maximal (Fig. 2A). YFP-N-β_1YFP-C-γ_1, the least effective complex, and YFP-N-β_1YFP-C-γ_{10}, the most effective complex, produced half-maximal plasma membrane targeting of α_s-CFP at intensities that were ~2- and ~3-fold greater, respectively, then when it was expressed alone (Fig. 2A, Table 1). The decreased effectiveness of YFP-N-β_1YFP-C-γ_1 was not due to a decreased amount of this complex, because its average intensity was similar to that of the other YFP-N-β_1YFP-C-γ complexes (Fig. 2B).

To normalize the α_s-CFP targeting abilities of the YFP-N-β_1YFP-C-γ complexes to their relative concentrations, the plasma membrane fraction of α_s-CFP was expressed as a function of the YFP-N-β_1YFP-C-γ to α_s-CFP intensity ratio in each cell (Fig. 2C). This ratio reflects the relative intracellular concentration of each of the different YFP-N-β_1YFP-C-γ complexes compared with that of α_s-CFP but is not a molar ratio of $\beta\gamma$ to α_s because the relative intensities of YFP produced by BiFC and of CFP have not been determined. Based on the YFP-N-β_1YFP-C-γ to α_s-CFP intensity ratio that resulted in half-maximal plasma membrane targeting of α_s-CFP, YFP-N-β_1YFP-C-γ_1 and YFP-N-β_1YFP-C-γ_{10} were still the least and most effective, respectively, at α_s-CFP targeting, differing by ~2-fold in their efficacies (Fig. 2C, Table 1). The decreased effectiveness of YFP-N-β_1YFP-C-γ_1 may be due in part to the fact that it exhibited somewhat less plasma membrane targeting itself than did the other $\beta\gamma$ dimers (Fig. 2D). The relatively low plasma membrane fractions of both YFP-N-β_1YFP-C-γ_1 and YFP-N-β_1YFP-C-γ_{11} (Fig. 2D) are consistent with the fact that γ_1 and γ_{11} are farnesylated, rather than geranylgeranylated like the other γ subunits tested here. Overall, however, the α_s-CFP targeting abilities of the different YFP-N-β_1YFP-C-γ complexes were fairly similar, suggesting that the corresponding $\beta_1\gamma$ complexes exhibit similar affinities for α_s.

Production of CFP-C-β_1CFP-N-γ Dimers for Use in Multicolor BiFC. Another potential source of functional diversity among G protein β and γ subunits could be preferential formation of particular $\beta\gamma$ complexes. To investigate this possibility, we chose to compare the abilities of γ_1, γ_2, γ_5, γ_7, γ_{10}, γ_{11}, and γ_{12} to compete for association with β_1 using multicolor BiFC (Hu and Kerppola, 2003). This approach consists of simultaneous visualization of the two fluorescent complexes formed when proteins fused to YFP-N and CFP-N interact with a common binding partner fused to CFP-C. Complexes containing YFP-N and CFP-C fusion proteins are yellow, whereas those containing CFP-N and CFP-C fusion proteins are cyan, because the amino terminal fragment of the fluorescent protein determines the spectral properties of the complex (Hu and Kerppola, 2003). We have produced YFP-N-βYFP-C-γ dimers previously (Hynes et al., 2004a,b) (Figs. 1 and 2). Now, to compare the interactions of different γ subunits with the same β subunit, we fused a carboxyl-terminal CFP fragment (residues 159–238) to β_1 to produce CFP-C-β_1, and amino-terminal CFP or YFP fragments (residues 1–158) to the γ subunits, producing CFP-N-γ and YFP-N-γ subunits (Fig. 3A).

Coexpression of CFP-C-β_1 with each of the CFP-N-γ subunits produced a fluorescent signal in the plasma membrane of HEK-293 cells that was not seen when individual subunits were expressed alone or when CFP-N and CFP-C were expressed together (Fig. 3B). These results indicate that the BiFC method can be applied to imaging $\beta\gamma$ complexes both when the amino terminal fragment of the fluorescent protein is attached to β and the carboxyl terminal fragment is attached to γ and vice versa. The intensities of the different complexes varied by 2-fold or less (Fig. 3C), indicating that CFP-C-β_1 interacts similarly with each of the CFP-N-γ subunits when coexpressed with one of them at a time. The plasma membrane fractions of each of the different CFP-C-β_1CFP-N-γ complexes, expressed in the absence of α_s-CFP, were similar (Fig. 3D) and were slightly less than those of YFP-N-β_1YFP-C-γ dimers coexpressed with α_s-CFP (Fig. 2D), suggesting that α_s plays a role in targeting $\beta\gamma$, as observed previously (Takida and Wedegaertner, 2003). However, this effect seems to be much slighter than that of $\beta\gamma$ on α_s targeting.

Seven CFP-N-γ Subunits Vary in Their Abilities to Compete with YFP-N-γ_2 for Association with CFP-C-β_1. Because it is likely that the predominance of particular $\beta\gamma$ dimers in individual cells is influenced by the relative association preferences of the expressed β and γ subunits, we postulated that preferential interactions between β_1 and particular γ subunits might be revealed when a limiting amount of CFP-C-β_1 was coexpressed with a CFP-N-γ and a YFP-N-γ. To test for this, we compared the abilities of each of the CFP-N-γ subunits to compete with YFP-N-γ_2 for binding to CFP-C-β_1 by measuring the cyan fluorescence (from a CFP-C-β_1CFP-N-γ complex) and yellow fluorescence (from CFP-C-β_1YFP-N-γ_2) obtained when CFP-C-β_1 was coexpressed with the CFP-N-γ subunit and YFP-N-γ_2. Figure 4A shows plots of YFP versus CFP intensity for individual HEK-293 cells transfected with equal amounts of plasmid encoding

either CFP-C-β_1 and YFP-N-γ_2 (red circles), CFP-C-β_1 and a CFP-N-γ subunit (blue circles,), or CFP-C-β_1, YFP-N-γ_2, and a CFP-N-γ subunit (green circles). Cells expressing only CFP-C-β_1 and YFP-N-γ_2 (Fig. 4A, red circles) or only CFP-C-β_1 and a CFP-N-γ subunit (Fig. 4A, blue circles), exclusively exhibited yellow or cyan fluorescence, respectively, whereas cells coexpressing CFP-C-β_1, YFP-N-γ_2, and a CFP-N-γ subunit (Fig. 4A, green circles), exhibited both yellow and cyan fluorescence. Under these transfection conditions, cells expressing CFP-C-β_1 and YFP-N-γ_2 exhibited an average yellow fluorescence intensity of 8.74 (S.E. = 0.48, n = 182), whereas cells expressing CFP-C-β_1 and CFP-N-γ_2 exhibited an average cyan fluorescence intensity of 9.53 (S.E. = 0.58, n = 178). Cells coexpressing CFP-C-β_1, YFP-N-γ_2, and CFP-N-γ_2 exhibited average yellow and cyan fluorescence intensities of 3.53 (S.E. = 0.21, n = 180) and 5.09 (S.E. = 0.25, n = 180), respectively, indicating that CFP-C-β_1 was limiting. Figure 4B shows representative cells expressing CFP-C-β_1YFP-N-γ_2, CFP-C-β_1CFP-N-γ_2, or both. Because $\beta\gamma$ complexes do not dissociate in the absence of denaturants (Clapham and Neer, 1997), except for $\beta_5\gamma$ complexes (Jones et al., 2004), the relative abilities of CFP-N-γ and YFP-N-γ subunits to compete for interaction with CFP-C-β_1 presumably reflect their abilities to associate with this β subunit. Differences in association could reflect variations in the affinities of the γ subunits for β_1, but other factors such as differential targeting to distinct cellular compartments or differences in interactions with chaperonins or other associated proteins (Clapham and Neer, 1997; Lukov et al., 2005; Li et al., 2006) could also regulate complex formation in vivo.

The fluorescence intensities of cells coexpressing CFP-C-β_1, YFP-N-γ_2, and a CFP-N-γ exhibited a linear relationship between the CFP and YFP intensities (Fig. 4A, green circles). This linearity suggests that the cells expressed each of the

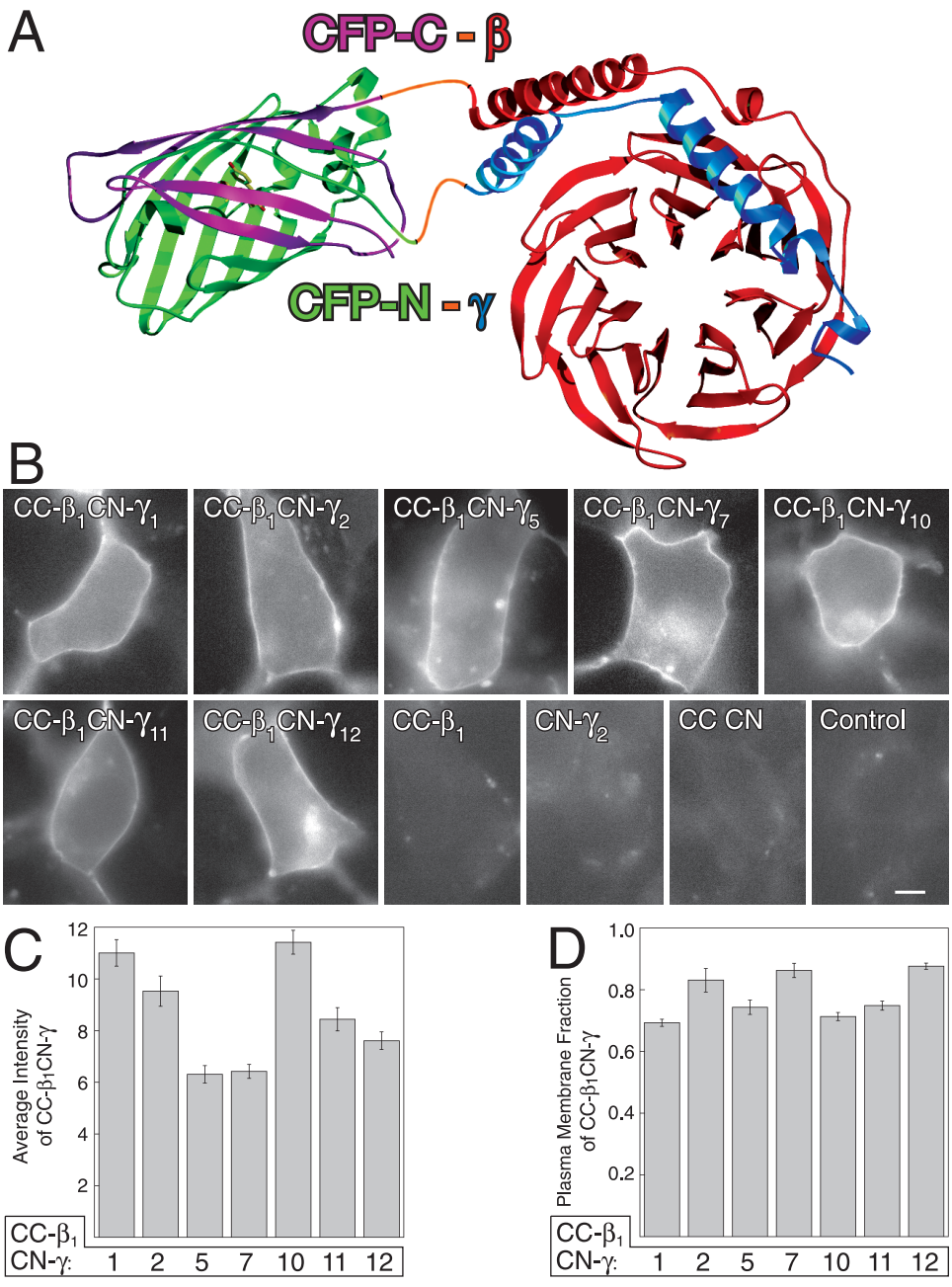

Fig. 3. Production of fluorescent $\beta_1\gamma$ complexes using BiFC for multicolor competition studies. A, model of CFP-C-βCFP-N-γ. The C-terminal CFP fragment, CFP(159–238), referred to as CFP-C (magenta), is fused to Gβ (red) and the N-terminal CFP fragment, CFP(1–158), referred to as CFP-N (green), which contains the chromophore, is fused to Gγ (blue). Linker sequences between the CFP fragments and the G protein subunits are orange. The structures of CFP-N and CFP-C are adapted from the structure of GFP (Ormo et al., 1996). The structures of β and γ are from the structure of an α_t/α_{i1} chimera complexed with $\beta_t\gamma_t$ (Lambright et al., 1996). B, CFP-C-β/CFP-N-γ dimers containing β_1 complexed with γ_1, γ_2, γ_5, γ_7, γ_{10}, γ_{11}, and γ_{12} exhibit similar plasma membrane localization patterns in HEK-293 cells. Cells were transfected with the indicated constructs and mRFP-Mem (membrane marker) as described under *Materials and Methods*. The control image is the CFP image of a cell expressing only mRFP-Mem. All images are 10-s exposures, and similar pixel ranges are displayed. CN indicates CFP-N and CC indicates CFP-C. Scale bar, 5 μm. C, average intensities of each of the CFP-C-β_1CFP-N-γ complexes. D, plasma membrane fractions of the CFP-C-β_1CFP-N-γ complexes. Values for C and D represent the means ± S.E of 147 to 243 measurements.

transfected plasmids in the same proportion, regardless of overall expression level, and also indicates that the abilities of the CFP-N-γ subunits to compete with YFP-N-γ_2 for association with CFP-C-β_1 were the same over the observed range of expression levels. The slopes of linear fits to these data indicate the relative abilities of the CFP-N-γ subunits to compete with YFP-N-γ_2 for dimerization with CFP-C-β_1, with the relative efficacies varying inversely with the slopes. These slope values spanned a range of ~5-fold (Fig. 4A). CFP-N-γ_2 was the most effective competitor, followed by CFP-N-γ_7. The other CFP-N-γ subunits were clearly less effective competitors.

To compare the abilities of the seven γ subunits to compete for β_1 more precisely, we measured the fluorescence intensities of populations of HEK-293 cells in a spectrofluorometer. This approach was justified by the linear relationship between YFP and CFP intensities of individual cells over a wide range of intensities (Fig. 4A) and made it possible to pool results from a much larger number of cells than was feasible by imaging individual cells (on the order of 10^6 compared with 10^2). This method made it possible to determine the relative amounts of each competitor that decreased the intensity of CFP-C-β_1YFP-N-γ_2 by 50%, enabling finer distinctions to be made among the set of γ subunits. For these experiments, we used a modified version of ECFP, referred to as Cerulean, which is 2.5-fold brighter than ECFP (Rizzo et al., 2004), to produce Cer-N-γ subunits. The fluorescence intensity of Cer-N-γ_2CFP-C-β_1 was 3.96-fold greater than that of CFP-N-γ_2CFP-C-β_1 (S.E. = 0.8, n = 3).

Cells were transfected with a range of amounts of Cer-N-γ subunit plasmids to enable determination of BiFC intensities and competitive abilities as a function of plasmid dose, keeping the total amount of plasmid constant with empty vector. In the presence of an excess of cotransfected CFP-C-β_1 plasmid, linear relationships between the amounts of transfected Cer-N-γ subunit plasmids and CFP-C-β_1Cer-N-γ intensities were obtained (Fig. 5A). The relative amounts of complexes formed between the different Cer-N-γ subunits and CFP-C-β_1, obtained from the slopes of linear fits to the data, varied by less than 3-fold, with CFP-C-β_1Cer-N-γ_2 and CFP-C-β_1Cer-N-γ_{12} exhibiting the greatest and least intensities, respectively (Table 2). Using an anti-GFP antibody, the relative expression levels of the Cer-N-γ subunits were determined by immunoblotting membranes from cells transfected in the same way as when BiFC intensities were compared (Fig. 5B). The relationship between Cer-N-γ subunit expression level and amount of transfected plasmid was also linear (Fig. 5C). The Cer-N-γ subunit expressed at the lowest level, Cer-N-γ_{12}, exhibited levels that were 21% of the one expressed at the highest level, Cer-N-γ_2 (Fig. 5D, Table 2). The ratios of the CFP-C-β_1Cer-N-γ intensities (Fig. 5A, Table 2) to the expression levels of the corresponding Cer-N-γ subunits (Fig. 5D, Table 2) were used to normalize the β_1-interacting abilities of the different γ subunits. These ratios

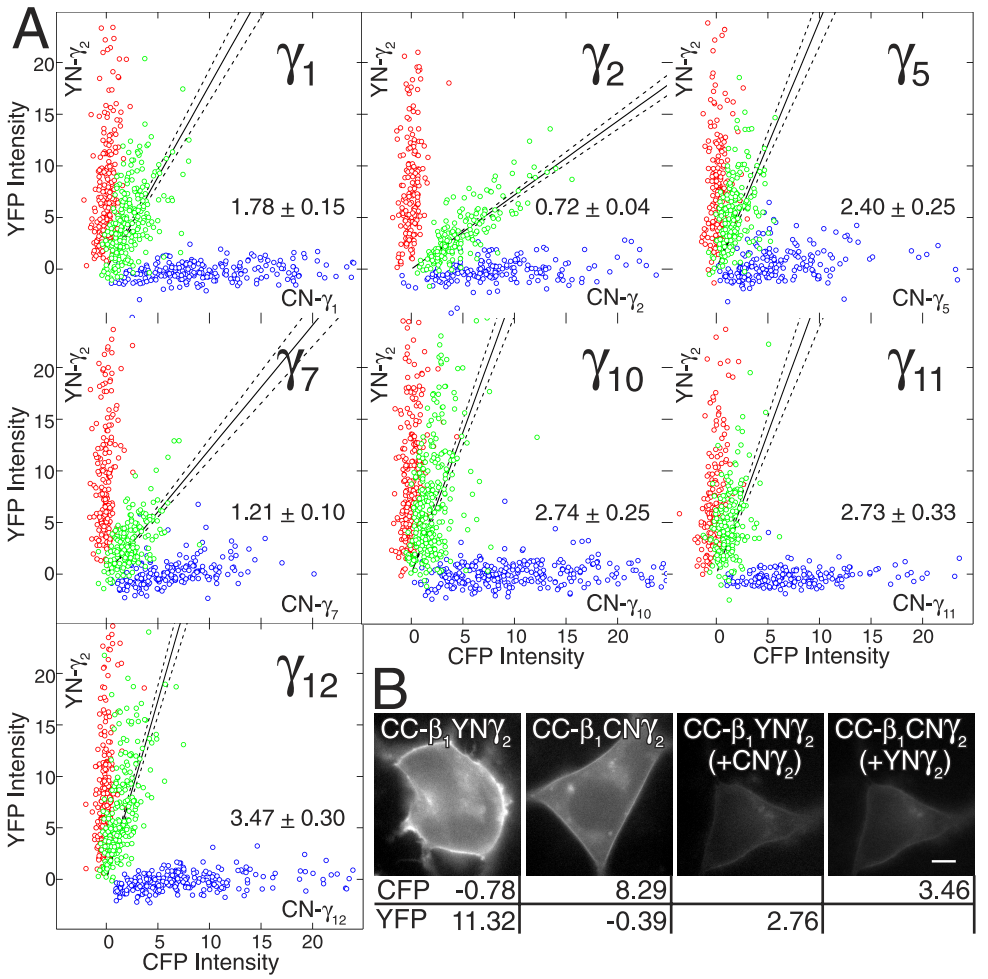

Fig. 4. Competition between different γ subunits to form complexes with β_1 using multicolor BiFC in individual microscopically imaged cells. HEK-293 cells were transfected as described under *Materials and Methods*. A, plots of YFP versus CFP intensity for individual cells transfected with plasmids encoding either CFP-C-β_1 and YFP-N-γ_2 (red), CFP-C-β_1 and a CFP-N-γ subunit (blue), or CFP-C-β_1, YFP-N-γ_2, and a CFP-N-γ subunit (green). One hundred seventy-eight to 310 cells were imaged for each condition. For clarity of presentation, only cells with intensities less than 25 are shown. The average autofluorescence signals in the YFP channel (1.36, S.E. = 0.03, n = 1390) and in the CFP channel (0.95, S.E. = 0.02, n = 1397), corresponding to the average intensity of cells transfected with CFP-C-β_1 and a CFP-N-γ subunit (blue) and CFP-C-β_1 and YFP-N-γ_2 (red), respectively, were subtracted before plotting and curve fitting. The linear fit of the competition data (green), calculated using Igor Pro (WaveMetrics, Inc., Lake Oswego, OR), is shown as a solid line with 95% confidence intervals indicated by dashed lines. B, representative images of cells expressing CFP-C-β_1YFP-N-γ_2 or CFP-C-β_1CFP-N-γ_2 alone and of the YFP and CFP signals in a cell coexpressing CFP-C-β_1, YFP-N-γ_2, and CFP-N-γ_2. The average CFP and YFP intensity values of the displayed cells are listed below the images. CN indicates CFP-N, YN indicates YFP-N, and CC indicates CFP-C. Scale bar, 5 μm.

were fairly similar, varying by 2-fold or less (Fig. 5E). These results, in agreement with the results from imaging individual cells (Figs. 2B and 3C), suggest that the abilities of different γ subunits to form complexes with β_1, when tested one at a time, are similar.

As was seen when the fluorescence intensities of individual cells were measured (Fig. 4), there were differences in the abilities of the Cer-N-γ subunits to compete with YFP-N-γ_2 for interaction with limiting amounts of CFP-C-β_1 in cell populations (Fig. 6). In agreement with the microscope stud-

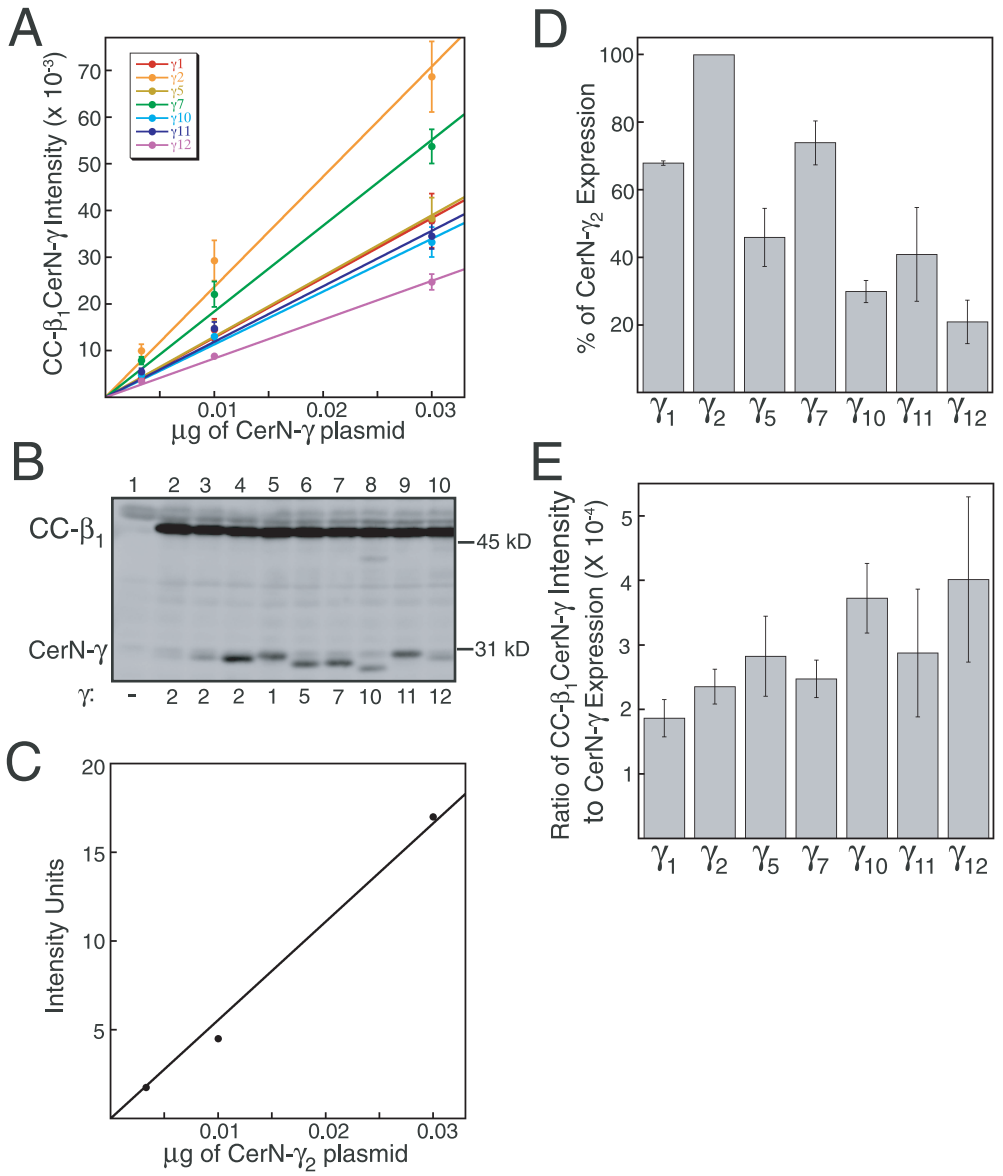

Fig. 5. Quantification of the fluorescence intensities of CFP-C-β_1Cer-N-γ complexes in cell populations. A, intensities of CFP-C-β_1Cer-N-γ complexes when CFP-C-β_1 is not limiting. HEK-293 cells (1.6×10^6 per 60-mm dish) were transfected with 2.4 μg of plasmid expressing CFP-C-β_1 and 0.0033, 0.01, or 0.03 μg of each Cer-N-γ subunit plasmid as indicated. The total amount of plasmid in each transfection was maintained at 2.43 μg by making up the difference with pcDNAI/Amp. Values represent the means ± S.E from three experiments performed in duplicate, and data were fit by linear regressions. CC indicates CFP-C. B, immunoblot showing expression levels of Cer-N-γ subunits. HEK-293 cells were transfected as in A, except that 100-mm dishes were used, and the number of cells and amounts of plasmids and Lipofectamine 2000 reagent were scaled up accordingly by a factor of 2.78. Membranes were prepared, resolved by SDS-polyacrylamide electrophoresis, and immunoblotted with a polyclonal antibody to GFP peptides as described under *Materials and Methods*. Lane 1 shows membranes from cells transfected with vector (pcDNAI/Amp). Lanes 2, 3, and 4 show membranes from cells transfected with plasmid expressing 2.4 μg of CFP-C-β_1 and 0.0033, 0.01, or 0.03 μg (per 1.6×10^6 cells) of Cer-N-γ_2, respectively. Membranes in lanes 5 to 10 are from cells transfected with 2.4 μg of CFP-C-β_1 and 0.03 μg (per 1.6×10^6 cells) of the indicated Cer-N-γ subunit. Similar results were obtained in two additional experiments. C, the expression level of Cer-N-γ_2 exhibited a linear relationship to the amount of transfected plasmid. The relative amounts of Cer-N-γ_2 protein in lanes 2 to 4 of the immunoblot in B were quantified as described under *Materials and Methods*. Similar results were obtained in two additional experiments. D, quantification of expression levels of Cer-N-γ subunits obtained from immunoblots. The relative expression levels of Cer-N-γ subunits in cells transfected with 2.4 μg of plasmid expressing CFP-C-β_1 and 0.03 μg of each Cer-N-γ subunit plasmid (per 1.6×10^6 cells) were quantified as described under *Materials and Methods* and are expressed as percentage of Cer-N-γ_2 expression. Values represent the means ± S.E from three experiments. E, normalization of CFP-C-β_1Cer-N-γ intensities to Cer-N-γ expression levels. The mean slopes of CFP-C-β_1Cer-N-γ intensity versus Cer-N-γ plasmid dose were divided by the relative expression levels of the corresponding to Cer-N-γ subunits, expressed as percentage of Cer-N-γ_2 expression (each from three experiments). The S.E. resulting from division of mean CFP-C-β_1Cer-N-γ intensity ± S.E. by Cer-N-γ expression level ± S.E. was calculated using an equation for error propagation (http://www.rit.edu/~uphysics/uncertainties/Uncertaintiespart2.html).

ies, Cer-N-γ_2 caused the largest decrease in intensity of CFP-C-β_1YFP-N-γ_2, followed by Cer-N-γ_7 (Fig. 6A, Table 2). The amount of Cer-N-γ_2 plasmid that reduced CFP-C-β_1YFP-N-γ_2 intensity by 50% was 15% of that of the weakest competitor, Cer-N-γ_{10} (Table 2). To control for Cer-N-γ expression levels, the plasmid amounts of these subunits were multiplied by their relative expression levels (Fig. 5D, Table 2). The most significant difference that resulted from this normalization was that Cer-N-γ_{12}, which was expressed at the lowest level of the Cer-N-γ subunits, became the most effective competitor (Fig. 6B, Table 2). In addition, the lower level of Cer-N-γ_{10} expression compared with that of Cer-N-γ_1 caused Cer-N-γ_1 to become the weakest competitor (Fig. 6B, Table 2). Thus, γ_1 was the least effective γ subunit both at competing for association with β_1 and, when complexed with β_1, at targeting α_s to the plasma membrane (Fig. 2, A and C). When expression levels were controlled for, Cer-N-γ_{12} was 4.5 times more effective at competing for association with CFP-C-β_1 than was Cer-N-γ_1 (Fig. 6B, Table 2).

Discussion

Previous studies of the specificity of G protein $\beta\gamma$ complex formation relied on comparisons of interactions between single pairs of β and γ subunits and generally were not conducted in intact mammalian cells. Given that cells coexpress multiple isoforms of β and γ, we sought to determine whether the predominance of particular $\beta\gamma$ complexes might be determined by the relative association preferences of the subunits.

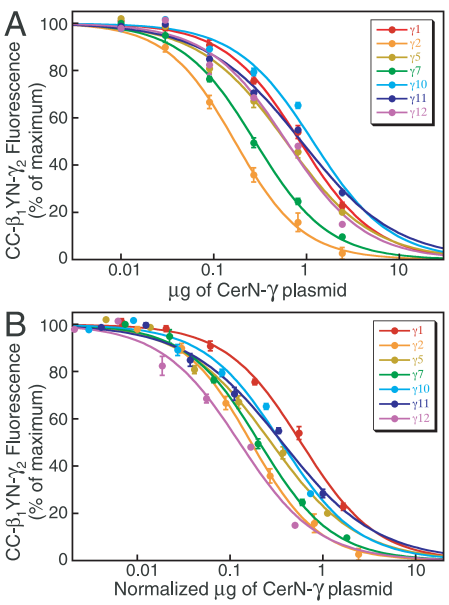

Fig. 6. Competition between Cer-N-γ and YFP-N-γ_2 subunits for limiting amounts of CFP-C-β_1 in cell populations. The intensity of CFP-C-β_1YFP-N-γ_2 was measured in the presence of a competing Cer-N-γ subunit or empty vector. HEK-293 cells were transfected with 0.6 μg each of plasmids expressing CFP-C-β_1 and YFP-N-γ_2, and 0, 0.01, 0.03, 0.09, 0.27, 0.81, or 2.43 μg of each Cer-N-γ subunit. The total amount of plasmid in each transfection was maintained at 3.63 μg by making up the difference with pcDNAI/Amp. YN indicates YFP-N, and CC indicates CFP-C. A, CFP-C-β_1YFP-N-γ_2 intensity expressed as a function of μg of cotransfected Cer-N-γ subunit plasmid. Values represent the means ± S.E. from three experiments performed in duplicate. B, CFP-C-β_1YFP-N-γ_2 intensity expressed as a function of the relative amounts of coexpressed Cer-N-γ subunits. The plasmid amounts of each of the Cer-N-γ subunits used in A were multiplied by their relative expression levels (fraction of the Cer-N-γ_2 level from Fig. 5D and Table 2).

We found that multicolor BiFC can be used to compare the abilities of different γ subunits to compete for limiting amounts of a shared β subunit in live cells. This strategy demonstrated a 4.5-fold range in the association preferences of β_1 for seven γ subunits. CFP-N-γ_{12} and CFP-N-γ_1 were the strongest and weakest competitors, respectively. Differences of this magnitude were not seen using single-color BiFC (in which each γ subunit was individually coexpressed with an excess of β_1), using the yeast two-hybrid system (Yan et al., 1996), immunoprecipitation of $\beta\gamma$ complexes from tissue extracts (Asano et al., 1999), or analysis of subunits synthesized in vitro using reticulocyte lysates (Schmidt et al., 1992; Ray et al., 1995; Dingus et al., 2005).

Preferential association of particular β and γ subunits is likely to be of functional importance in regulating interactions between G protein-coupled receptors and G proteins. For instance, ribozyme-mediated suppression of γ_7 in HEK-293 cells specifically reduced expression of β_1 and disrupted activation of G_s by β-adrenergic and D_1 dopamine receptors, but not by prostaglandin E_1 and D_5 dopamine receptors (Wang et al., 1997, 1999, 2001). In mice lacking γ_7, D_1 dopamine receptor-mediated stimulation of adenylyl cyclase activity in the striatum was lost (Schwindinger et al., 2003). Moreover, an in vitro study comparing the abilities of $\alpha_{i1}\beta_1\gamma$ complexes to produce high affinity agonist binding to the α_{2a}-adrenergic receptor showed that complexes containing γ_2, γ_3, γ_4, γ_7, and γ_{11} were ~3 times more effective than complexes containing γ_5 and γ_{10}, and ~30 times more effective than $\alpha_{i1}\beta_1\gamma_1$ (Richardson and Robishaw, 1999). Another study comparing the abilities of $\alpha_{i1}\beta_1\gamma$ complexes containing γ_1, γ_2, γ_7, γ_{10}, or γ_{11} to produce high affinity agonist binding to α_{2a}-adrenergic, A1 adenosine, 5-hydroxytryptamine$_{1A}$, and μ-opioid receptors found a 3- to 8-fold range in potencies; $\alpha_{i1}\beta_1\gamma_{11}$ was the most effective for A1 adenosine and 5-hydroxytryptamine$_{1A}$ receptors and $\alpha_{i1}\beta_1\gamma_7$ was the most potent for the α_{2a}-adrenergic and μ-opioid receptors (Lim et al., 2001). In addition, the magnitude of activation of $\alpha_{i1}\beta_4\gamma_2$ by endogenous α_2-adrenergic receptors in HeLa cells was 3 times that of $\alpha_{i1}\beta_2\gamma_2$ as determined by FRET analysis (Gibson and Gilman, 2006) and $\beta_4\gamma_2$ was 12 times more effective than $\beta_1\gamma_2$ at coupling G_s to the A2a adenosine receptor in a reconstituted system (McIntire et al., 2001).

The role of $\beta\gamma$ in mediating specificity at the level of interactions with α subunits and effectors, compared with receptors, may be more variable. Regarding α subunit interaction, we did not observe large differences in the abilities of $\beta_1\gamma$ complexes to target α_s-CFP to the plasma membrane. $\beta_1\gamma_1$ was ~2-fold less effective than $\beta_1\gamma_{10}$, the most effective complex, but it also exhibited less plasma membrane targeting itself. It is possible that greater differences might have been seen among a wider selection of $\beta\gamma$ dimers in interactions with α_s as well as with other α subunits. For instance, a previous study examined the ability of β_{1-5} in combination with γ_2 or γ_3 to promote plasma membrane targeting of $\beta\gamma$-binding deficient mutants of α_s and α_q (Evanko et al., 2001) and found that whereas $\beta_1\gamma_3$ was equally effective as $\beta_1\gamma_2$ at targeting mutant α_s, $\beta_5\gamma$ and $\beta_3\gamma$ complexes were ineffective and weak, respectively, and $\beta_4\gamma$ complexes effectively targeted mutant α_s but not mutant α_q. The preferences of α subunits and $\beta\gamma$ complexes for each other in targeting assays could be due to differences in relative affinities, accessibilities, or other cellular factors. Direct comparisons of

the affinities of α and $\beta\gamma$ subunits for each other are more readily carried out in vitro. For instance, a comparison of the abilities of $\beta_1\gamma$ complexes containing γ_1, γ_2, γ_7, γ_{10}, or γ_{11} to compete for binding to fluorescein-labeled α_{i1} in a flow cytometry assay demonstrated that $\beta_1\gamma_1$ was 2- to 5-fold less potent than the other complexes (Lim et al., 2001). At the level of effector interaction, many $\beta\gamma$ combinations exhibit similar abilities to modulate effector proteins (Iniguez-Lluhi et al., 1992), although preferential interactions have been seen (McIntire et al., 2001). In addition, effector regulation by $\beta\gamma$ in vivo can be more selective than that in vitro (Diverse-Pierluissi et al., 2000). Moreover, the pronounced phenotypes obtained using targeted deletions of γ subunits (Schwindinger et al., 2003, 2004) suggest that differences in the interactions of $\beta\gamma$ subunits with receptors, α subunits, and effectors, although not always robust when examined individually, may have additive effects that lead to a high degree of signaling specificity.

The ability of multicolor BiFC to determine preferences in the formation of particular $\beta\gamma$ complexes in live cells is advantageous because in vivo factors can affect $\beta\gamma$ assembly. For instance, the 90-kDa heat shock protein can be immunoprecipitated with nondimerized β subunits but not $\beta\gamma$ complexes (Clapham and Neer, 1997); binding of phosducin-like protein to β_1 is required for association with γ_2 in vivo (Lukov et al., 2005), and an immature form of γ_{13} interacts with PDZ-containing proteins (Li et al., 2006). It is possible that coexpression of phosducin or another retina-specific chaperonin might cause γ_1, which interacts with β_1 in the retina, to compete more effectively for β_1 in HEK-293 cells. In addition, relationships between subcellular compartmentalization and association of particular β and γ subunits can only be investigated using intact cells. γ_5 can associate with focal adhesions (Hansen et al., 1994), whereas γ_{12} can associate with actin filaments (Ueda et al., 1997). Application of BiFC will enable determination of the β subunits with which these γ subunits are associated and may demonstrate differential localization patterns depending on the associated β subunit. For instance, we found previously that $\beta_5\gamma$ complexes localize to the cytoplasm, either diffusely or on intracellular membranes, depending on the associated γ subunit, whereas the corresponding $\beta_1\gamma$ complexes localize to the plasma membrane (Hynes et al., 2004b).

Comparing the abilities of additional β and γ subunits to interact with each other using multicolor BiFC will provide a more comprehensive picture of which complexes are likely to predominate in particular cells. For instance, the presence of other β subunits will affect which γ subunits interact preferentially with β_1. Based on analysis of the subunit composition of $\beta\gamma$ complexes purified from bovine tissues, γ_5 and γ_{12} seem to associate selectively with β_4 (Asano et al., 1999). If γ_{12} interacts preferentially with β_4 rather than β_1, this could explain why γ_{12} could not prevent a decrease in the level of β_1 upon ribozyme-mediated depletion of γ_7 in HEK-293 cells (Wang et al., 1997). It is not clear why γ_2, which also competed for β_1 more effectively, could not substitute for γ_7, but it is possible that γ_2 is expressed at a lower level or interacts preferentially with a different β subunit in HEK-293 cells. To address such questions, multicolor BiFC can be applied to additional analyses of γ subunits competing for β subunits as well as of β subunits competing for γ subunits.

Cell-type specific patterns of β and γ expression, as well as their association preferences, will determine which $\beta\gamma$ complexes predominate in particular cells. For instance, γ_5 and γ_{12} are the major γ subunits in HEK-293, HeLa, and BRL-3A cells, whereas γ_2 and γ_5 prevail in F9 and NG108-15 cells (Ueda et al., 1998). In addition, differences in γ expression levels have been observed during development. One study found that retinoic acid-induced differentiation of HL-60 cells into neutrophil-like cells involves induction of γ_2 expression and potentiation of fMLP stimulation of phospholipase C via G_i (Iiri et al., 1995). Another study found that γ_5 is the predominant γ subunit in undifferentiated HL-60 cells, and retinoic acid-induced differentiation induces expression of both γ_2 and γ_7, with γ_2 replacing most of the γ_5 (Ueda et al., 1998). Likewise, γ_2 replaces γ_5 during neuronal differentiation in rat brain (Morishita et al., 1999). Because interactions between specific G protein subunits seem to be important for mutual stabilization (Wang et al., 1999; Schwindinger et al., 2003), alterations in the expression of particular subunits may cause changes in the levels of their binding partners.

Taken together with demonstrations that targeted deletions of specific γ subunits can produce unique effects and that both α and $\beta\gamma$ composition play a role in determining receptor specificity, our results showing preferences of β_1 for particular γ subunits suggest that multiple levels of selective interactions contribute to G protein signaling specificity. Combining diverse approaches to compare the expression levels of the G protein subunits, their preferences for association, and the preferences of G protein-coupled receptors for particular $\alpha\beta\gamma$ heterotrimers will elucidate which complexes are most likely to form in a particular cellular environment and mediate specific signaling pathways.

Acknowledgments

We thank David Piston for the monomeric cerulean plasmid, Roger Tsien for the monomeric RFP1 plasmid, Janet Robishaw for plasmids expressing β and γ subunits, and Gerda Breitwieser for helpful discussions and critical reading of the manuscript.

References

Asano T, Morishita R, Ueda H, and Kato K (1999) Selective association of G protein β_4 with γ_5 and γ_{12} subunits in bovine tissues. *J Biol Chem* **274:**21425–21429.

Clapham DE and Neer EJ (1997) G protein beta gamma subunits. *Annu Rev Pharmacol Toxicol* **37:**167–203.

Dingus J, Wells CA, Campbell L, Cleator JH, Robinson K, and Hildebrandt JD (2005) G protein betagamma dimer formation: Gbeta and Ggamma differentially determine efficiency of in vitro dimer formation. *Biochemistry* **44:**11882–11890.

Diverse-Pierluissi M, McIntire WE, Myung CS, Lindorfer MA, Garrison JC, Goy MF, and Dunlap K (2000) Selective coupling of G protein $\beta\gamma$ complexes to inhibition of Ca^{2+} channels. *J Biol Chem* **275:**28380–28385.

Evanko DS, Thiyagarajan MM, Siderovski DP, and Wedegaertner PB (2001) G$\beta\gamma$ isoforms selectively rescue plasma membrane localization and palmitoylation of mutant Gα_s and Gα_q. *J Biol Chem* **276:**23945–23953.

Evanko DS, Thiyagarajan MM, and Wedegaertner PB (2000) Interaction with G$\beta\gamma$ is required for membrane targeting and palmitoylation of Gα_s and Gα_q. *J Biol Chem* **275:**1327–1336.

Figler RA, Lindorfer MA, Graber SG, Garrison JC, and Linden J (1997) Reconstitution of bovine A1 adenosine receptors and G proteins in phospholipid vesicles: betagamma-subunit composition influences guanine nucleotide exchange and agonist binding. *Biochemistry* **36:**16288–16299.

Gibson SK and Gilman AG (2006) Gialpha and Gbeta subunits both define selectivity of G protein activation by alpha2-adrenergic receptors. *Proc Natl Acad Sci USA* **103:**212–217.

Hansen CA, Schroering AG, Carey DJ, and Robishaw JD (1994) Localization of a heterotrimeric G protein gamma subunit to focal adhesions and associated stress fibers. *J Cell Biol* **126:**811–819.

Hou Y, Azpiazu I, Smrcka A, and Gautam N (2000) Selective role of G protein γ subunits in receptor interaction. *J Biol Chem* **275:**38961–38964.

Hu CD, Chinenov Y, and Kerppola TK (2002) Visualization of interactions among bZIP and Rel family proteins in living cells using bimolecular fluorescence complementation. *Mol Cell* **9:**789–798.

Hu CD and Kerppola TK (2003) Simultaneous visualization of multiple protein interactions in living cells using multicolor fluorescence complementation analysis. *Nat Biotechnol* **21:**539–545.

Hynes TR, Mervine SM, Yost EA, Sabo JL, and Berlot CH (2004a) Live cell imaging of G_s and the β_2-adrenergic receptor demonstrates that both α_s and $\beta_1\gamma_7$ internalize upon stimulation and exhibit similar trafficking patterns that differ from that of the β_2-adrenergic receptor. *J Biol Chem* **279:**44101–44112.

Hynes TR, Tang L, Mervine SM, Sabo JL, Yost EA, Devreotes PN, and Berlot CH (2004b) Visualization of G protein $\beta\gamma$ dimers using bimolecular fluorescence complementation demonstrates roles for both β and γ in subcellular targeting. *J Biol Chem* **279:**30279–30286.

Iiri T, Homma Y, Ohoka Y, Robishaw JD, Katada T, and Bourne HR (1995) Potentiation of G_i-mediated phospholipase C activation by retinoic acid in HL-60 cells. Possible role of $G\gamma_2$. *J Biol Chem* **270:**5901–5908.

Iniguez-Lluhi JA, Simon MI, Robishaw JD, and Gilman AG (1992) G protein $\beta\gamma$ subunits synthesized in Sf9 cells. Functional characterization and the significance of prenylation of γ. *J Biol Chem* **267:**23409–23417.

Jones MB, Siderovski DP, and Hooks SB (2004) The G{beta}{gamma} dimer as a novel source of selectivity in G-protein signaling: GGL-ing at convention. *Mol Interv* **4:**200–214.

Lambright DG, Sondek J, Bohm A, Skiba NP, Hamm HE, and Sigler PB (1996) The 2.0 Å crystal structure of a heterotrimeric G protein. *Nature (Lond)* **379:**311–319.

Li Z, Benard O, and Margolskee RF (2006) Gγ13 interacts with PDZ domain-containing proteins. *J Biol Chem* **281:**11066–11073.

Lim WK, Myung CS, Garrison JC, and Neubig RR (2001) Receptor-G protein gamma specificity: gamma11 shows unique potency for A(1) adenosine and 5-HT(1A) receptors. *Biochemistry* **40:**10532–10541.

Lukov GL, Hu T, McLaughlin JN, Hamm HE, and Willardson BM (2005) Phosducin-like protein acts as a molecular chaperone for G protein betagamma dimer assembly. *EMBO (Eur Mol Biol Organ) J* **24:**1965–1975.

McIntire WE, MacCleery G, and Garrison JC (2001) The G protein β subunit is a determinant in the coupling of G_s to the β_1-adrenergic and A2a adenosine receptors. *J Biol Chem* **276:**15801–15809.

Morishita R, Shinohara H, Ueda H, Kato K, and Asano T (1999) High expression of the gamma5 isoform of G protein in neuroepithelial cells and its replacement of the gamma2 isoform during neuronal differentiation in the rat brain. *J Neurochem* **73:**2369–2374.

Ormo M, Cubbitt AB, Kallio K, Gross LA, Tsien RY, and Remington SJ (1996) Crystal structure of the *Aequoria victoria* green fluorescent protein. *Science (Wash DC)* **273:**1392–1395.

Ostrom RS (2002) New determinants of receptor-effector coupling: trafficking and compartmentation in membrane microdomains. *Mol Pharmacol* **61:**473–476.

Ray K, Kunsch C, Bonner LM, and Robishaw JD (1995) Isolation of cDNA clones encoding eight different human G protein γ subunits, including three novel forms designated the γ4, γ10 and γ11 subunits. *J Biol Chem* **270:**21765–21771.

Richardson M and Robishaw JD (1999) The α_{2A}-adrenergic receptor discriminates between G_i heterotrimers of different $\beta\gamma$ subunit composition in Sf9 insect cell membranes. *J Biol Chem* **274:**13525–13533.

Rizzo MA, Springer GH, Granada B, and Piston DW (2004) An improved cyan fluorescent protein variant useful for FRET. *Nat Biotechnol* **22:**445–449.

Robishaw JD and Berlot CH (2004) Translating G protein subunit diversity into functional specificity. *Curr Opin Cell Biol* **16:**206–209.

Schmidt CJ, Thomas TC, Levine MA, and Neer EJ (1992) Specificity of G protein β and γ subunit interactions. *J Biol Chem* **267:**13807–13810.

Schwindinger WF, Betz KS, Giger KE, Sabol A, Bronson SK, and Robishaw JD (2003) Loss of G protein γ_7 alters behavior and reduces striatal α_{olf} level and cAMP production. *J Biol Chem* **278:**6575–6579.

Schwindinger WF, Giger KE, Betz KS, Stauffer AM, Sunderlin EM, Sim-Selley LJ, Selley DE, Bronson SK, and Robishaw JD (2004) Mice with deficiency of G protein gamma3 are lean and have seizures. *Mol Cell Biol* **24:**7758–7768.

Takida S and Wedegaertner PB (2003) Heterotrimer formation, together with isoprenylation, is required for plasma membrane targeting of G$\beta\gamma$. *J Biol Chem* **278:**17284–17290.

Ueda H, Morishita R, Katoh-Semba R, Kato K, and Asano T (1998) G protein gamma subunits coimmunoprecipitated with antibodies against alpha subunits: identification of major isoforms in cultured cells by silver stain and immunoblotting with conventional transfer procedure. *J Biochem (Tokyo)* **124:**1033–1037.

Ueda H, Saga S, Shinohara H, Morishita R, Kato K, and Asano T (1997) Association of the gamma12 subunit of G proteins with actin filaments. *J Cell Sci* **110:**1503–1511.

Wang Q, Jolly JP, Surmeier JD, Mullah BM, Lidow MS, Bergson CM, and Robishaw JD (2001) Differential dependence of the D1 and D5 dopamine receptors on the G protein γ_7 subunit for activation of adenylylcyclase. *J Biol Chem* **276:**39386–39393.

Wang Q, Mullah B, Hansen C, Asundi J, and Robishaw JD (1997) Ribozyme-mediated suppression of the G protein γ_7 subunit suggests a role in hormone regulation of adenylylcyclase activity. *J Biol Chem* **272:**26040–26048.

Wang Q, Mullah BK, and Robishaw JD (1999) Ribozyme approach identifies a functional association between the G protein $\beta_1\gamma_7$ subunits in the β-adrenergic receptor signaling pathway. *J Biol Chem* **274:**17365–17371.

Wedegaertner PB, Wilson PT, and Bourne HR (1995) Lipid modifications of trimeric G proteins. *J Biol Chem* **270:**503–506.

Yan K, Kalyanaraman V, and Gautam N (1996) Differential ability to form the G protein $\beta\gamma$ complex among members of the β and γ subunit families. *J Biol Chem* **271:**7141–7146.

Address correspondence to: Catherine Berlot, Weis Center for Research, Geisinger Clinic, 100 North Academy Avenue, Danville, PA 17822-2623. E-mail: chberlot@geisinger.edu